Quality & Quantity
https://doi.org/10.1007/s11135-024-01975-x

Mathematical model of COVID-19 dynamics in the presence of multiple controls

J. O. Akanni[1,2] · Fatmawati[2] · S. Ajao[3] · J. K. K. Asamoah[4,5] · S. F. Abimbade[6]

Accepted: 30 August 2024

Abstract
The coronavirus disease 19 (COVID-19), caused by the Severe Acute Respiratory Syndrome Coronavirus 2 (SARS-COV-2), is an infectious disease constituting the most significant challenge to human and socio-economic development across the globe. Many studies have been conducted to gain more knowledge on the dynamic spread of SARS-COV-2 in the community of people. In this study, a new mathematical model made up of a system of non-linear ODEs is designed and meticulously analyzed to understand the dynamics of transmission of COVID-19. Specific necessary properties exhibited by the COVID-19 model are examined through the theory of non-negativity and boundedness of solutions. The threshold parameter measuring the invasion potential of COVID-19 in the population is worked out by employing the Next Generation Matrix approach. The model is shown to have two endemic equilibria whenever basic reproduction number $\mathcal{R}_0 < 1$. The analysis of the endemic equilibrium stability is explored using a suitably constructed Lyapunov function. It is shown that the COVID-19 model is globally asymptotically stable whenever the associated basic reproduction number is beyond unity. The Latin Hypercube Sampling or Partial Rank Correlation Coefficient is utilized to examine how parameter changes affect the COVID-19 spread in the population. Furthermore, the study considers six optimal control interventions to flatten the curve of the coronavirus pandemic in society. Numerical experiments of the COVID-19 model are executed in MatLab to corroborate the qualitative analysis of the model.

Keywords Mathematical modelling · COVID-19 · Dynamical system · Sensitivity analysis · LHS/PRCC · Optimal control analysis · cost-effectiveness analysis

Mathematics Subject Classification 49J15

1 Introduction

Coronavirus disease is a contagious disease otherwise known as COVID-19. The Severe Acute Respiratory Syndrome Coronavirus-2 (SARS-CoV-2) is the causative agent responsible for this deadly infection. It is not news anymore that COVID-19 is a disease of global concern due to the atrocity COVID-19 has wreaked on the general populace. It was

Extended author information available on the last page of the article

reported that approximately 760 million people got ill with the disease, with over 6.9 million deaths globally since its emergence in December 2019 (World Health Organization 2024; Centre for Disease Control and Prevention 2024). Coronavirus disease is primarily transmitted among individuals sharing a common closed environment through the droplets or aerosols deposited in the surroundings when an infected person speaks, sneezes, breathes, coughs or sings (Kouidere et al. 2023; Garba et al. 2020; Tang et al. 2020). COVID-19 may be contracted by any individual and become seriously sick or die depending on the immunity of the infected individual. At the same time, people may recover from the disease without any medical intervention. Individuals above 60 years of age and those with underlying ailments are most vulnerable to COVID-19, and symptoms may be fatal if control efforts are not sought early enough to combat the disease (Masandawa et al. 2021). The deadly coronavirus disease is characterized by different categories of symptoms, with sore throat, chills, and fever being the most common, while severe fatigue, dizziness, sore eyes, sneezing, breathing problems, tingling and loss of sense of smell or taste to mention. Still, a few are the less common symptoms (World Health Organization 2024; Centre for Disease Control and Prevention 2024; Abriham et al. 2021; Abidemi et al. 2021).

The vaccine against COVID-19 was recently invented in January 2021 to fight against the coronavirus dynamics in the population (Mekonen et al. 2023; Paul et al. 2023; Yang et al. 2022). In March 2023, the World Health Organization recommended using primary series vaccination (i.e. use of any two doses of vaccine) and booster doses to fight COVID-19 dynamics in the population (Huang et al. 2021). Vaccination against COVID-19 is time-constrained depending on the invasion potential of coronavirus in the population and potency of the vaccine. An estimated 13 billion vaccines have been administered as of June 2023 to forestall the COVID-19 spread globally (Mekonen et al. 2023). The intervention of vaccines against the infection has mitigated the COVID-19 spread by rescuing millions of lives from the threat posed by COVID-19 in the population through preservation against severe disease, hospitalization, and death. Inoculation against COVID-19 does not guarantee total recovery as there is every likelihood that vaccinated individuals who are still harbouring COVID-19 may transmit the disease (Srivastav et al. 2021; Ferguson et al. 2020).

To understand the complexities relating to SARS-CoV-2 transmission in the population, efforts have been made by several researchers and scientists around the globe using a variety of approaches. Particularly in epidemiology, mathematical modelling has become a vital tool in understanding the mechanism behind the dynamical spread of SARS-CoV-2. In addition, mathematical models focused mainly on compartmental models, which can be defined as the sub-categorization of the overall population at time, t, into various classes. Compartmental models are considerable tools used in battling problem formulations due to their ability to describe disease transmission patterns precisely. To this end, various multigroup models have been designed to explore the transmission dynamics of SARS-CoV-2 and other diseases in a locality. A stochastic model of HIV/AIDS was formulated by Zhai et al. (2023), which incorporates the susceptible individuals who are aware of the protective measures. The study's results revealed that increasing the efficacy of protecting susceptible individuals with protection awareness would reduce the infected persons' scale. Also, using antiretroviral therapy continuously can control the population of infected persons. The media reports that focus on the use of post-exposure prophylaxis can subdue the infection spread. The study of the application of optimal control to the recurrent situation of malaria was carried out by Olaniyi et al. (2023). The numerical experiments carried out express the impacts of doubling optimal control functions on the malaria recurrent situation. The work of Balakrishnan and Varadharajan (2024) deals with a multilevel model of Paediatric TB and a spatial method was used to detect 62 hotspots in India. The model

showed a nested structure, with states and districts contributing greatly to the changes in paediatric tuberculosis, and the autocorrelation pattern shown by the hotspots emphasizes the need for targeted tuberculosis eradication programmes.

Authors in Okuonghae and Omame (2020), Olaniyi et al. (2020), Asamoah et al. (2020), Goswami and Shanmukha (2021), Khan et al. (2022), Asamoah et al. (2022), Kifle and Obsu (2022), Li and Guo (2022), Rai et al. (2023), Das et al. (2023), Sharbayta et al. (2023), Rois et al. (2023), Abidemi et al. (2023), Idisi et al. (2023) have worked on the modelling of COVID-19. In Okuonghae and Omame (2020), the authors investigated the influence of certain interventions that are not pharmaceutical on the dynamical transmission of SARS-CoV-2 through the implementation of a deterministic mathematical model. The designed model was calibrated to Lagos State, Nigeria's COVID-19 active cases data.

Olaniyi et al. (2020) rigorously studied the dynamics of coronavirus disease spread by considering three transmission means, including symptomatic, asymptomatic, and hospitalized people. The model was calibrated to the number of cumulative cases of COVID-19 in Nigeria. The analysis was further extended to incorporate two time-dependent optimal controls to curb COVID-19 spread in the population. Authors in Asamoah et al. (2020) designed and analyzed a robust mathematical model incorporating environmental effects on the coronavirus disease transmission dynamics. The authors extended the developed model to accommodate control strategies explored using the theory of optimal control, and economic analysis was employed to determine the most cost-effective approach that would best avert the highest number of COVID-19 cases in the population. The authors concluded that the non-pharmaceutical intervention strategy is the most economical approach that best averts the highest number of infections in the community among all the intervention strategies competing for the same goal.

In another development, a mathematical model featuring the combined effect of vaccine efficacy and environmental factors on the spread of COVID-19 was studied in Rai et al. (2023). Similarly, Das et al. (2023) investigated the immigration and emigration effects of the infected individuals on COVID-19 transmission with environmental factors. Sharbayta et al. (2023) stressed the influence of double-dose vaccination on the coronavirus dynamics using a mathematical framework based on a system of ODEs. The study stratified the formulated model into two categories: the vaccination and no-vaccination models. The model was rigorously analyzed, concluding that efforts should be intensified in vaccinating individuals to successfully forestall the coronavirus disease menace. In a study by Rois et al. (2023), a new mathematical model classifying the total human population was developed, and the classes comprised the isolated infected individuals who were treated and isolated infected individuals without treatment regimes. The study considered a single optimal control intervention representing a public education programme to subdue COVID-19 using optimal control theory. Abidemi et al. (2023) explored the influence of COVID-19 on higher education in developing countries. The authors in Idisi et al. (2023) crafted a robust mathematical model to understand the transmission mechanism of the alpha variant of coronavirus in Nigeria. The effects of vaccination and certain non-pharmaceutical approaches were taken into account to provide lasting solutions to the ongoing pandemic. For further details on the SARS-CoV-2 dynamical transmission in the population, readers may see the following recent works and the references cited therein Iyaniwura et al. (2023), Sepulveda et al. (2023), Venkatesh et al. (2023), Awasthi (2023), Haq et al. (2023). Also, hen et al. (2021) studied the optimal control analysis of a COVID-19 model with vaccination, with four control strategies being deployed into the model. However, the SARS-CoV-2 transmission from an acutely infected individual is limited in the literature. This study, therefore, designs a new mathematical model considering

acutely infected individuals capable of transmitting COVID-19, intending to provide suggestions that will assist the general populace in utterly mitigating the invasion of the Coronavirus in society. The model's scope was expanded to incorporate six time-dependent optimal control interventions, and the non-autonomous part was analyzed using the celebrated Pontryagin maximum principle.

Further presentation of the study is structured as follows: Sect. 2 is dedicated to the formation of the COVID-19 model, and the investigation of basic properties exhibited by the COVID-19 model is explored in Sect. 3; In Sect. 4, the stability analysis is explored and it also consists of the determination of the disease-free equilibrium and basic reproduction number of the COVID-19 model, the investigation of the endemic equilibrium point of the model and the global stability of the model around the endemic equilibrium point is examined through a suitably constructed Lyapunov functions; Sect. 5 has the presentation of how changes in parameters of the model affect the disease outbreak; In Sect. 6, the proposed COVID-19 model was extended to accommodate optimal control sextuple. The study ended with a conclusion in Sect. 7.

2 Formation of the coronavirus model

The whole human population at time t, denoted by $N(t)$, is subdivided into six mutually disjointed classes of susceptible $S(t)$, exposed $E(t)$, acutely infected $A(t)$, infectious $I(t)$, hospitalized $H(t)$ and recovered $R(t)$, so that: $N(t) = S(t) + E(t) + A(t) + I(t) + H(t) + R(t)$. The population $S(t)$ is formed by recruiting new active individuals (assumed susceptible) into the community at a rate Λ. This population is decreased by the standard incidence rate $\frac{\beta(I(t)+\eta A(t))}{N}$, where η is the modification parameter based on the assumption that acutely infected individuals have a lesser chance of being infectious compared to infectious individuals, and β is the effective infection rate. The population $(E(t))$ comprises newly infected persons at the rate $\frac{\beta(I(t)+\eta A(t))}{N}$. This class size decreases due to progression to $A(t)$ and $I(t)$ classes at rates ε and θ, respectively. The population $(A(t))$ grows by the progression of infected people from $E(t)$ compartment at a rate ε. The size of the class is further diminished due to the progression of individuals to the $I(t)$ class at a rate ψ, $H(t)$ class at a rate ϕ, and $R(t)$ class at a rate κ, accordingly. The population of $(I(t))$ is proliferated by the movement of COVID-19 infectious people from the compartments $E(t)$ and $A(t)$ at rates θ and ψ receptively. The population reduces following the progression of individuals to $H(t)$ class at a rate ω. The class is further downsized at a rate δ representing coronavirus-induced death. The class of individuals in the isolation centre, $(H(t))$, is generated from the progressions of acutely infected individuals, $A(t)$, at a rate ϕ, infectious individuals, $I(t)$, at a rate ω. It decreases by recovery of infected people at a rate (ρ). The coronavirus-induced death rate δ further reduces the compartment size. Furthermore, the population class of $(R(t))$ of those who are cured of the deadly disease is increased by movement from $A(t)$ and $H(t)$ classes at rates κ and ρ, respectively. The overall human population $(N(t))$ diminishes by the natural mortality at rate μ. Consequently, the classical-order mathematical model portraying the transmission dynamics of the coronavirus disease is given in subsection 2.1.

Table 1 Meaning of the variables of model (1)

Parameter	Variable	Parameter	Variable
S	Susceptible class	E	Exposed class
A	COVID-19 Acutely-infected class	I	Infectious class
H	Hospitalized class	R	Recovered class

Table 2 Meaning of each parameter of the model (1)

Parameter	Description	Parameter	Description
Λ	Constant recruitment rate	β	COVID-19 transmission rate
η	Modification parameter for A(t)	μ	Natural mortality rate
ε	Movement rate from E(t) to A(t)	θ	Movement rate from E(t) to I(t)
ψ	Movement rate from A(t) to I(t)	ϕ	Hospitalized rate of A(t)
κ	Recovery rate of A(t)	δ	Induced mortality rate
ω	Hospitalized rate of I(t)	ρ	Recovery Rate of H(t)

2.1 Model with no COVID-19 infection control formulation

Here, the autonomous system of equations representing the time-evolution of the SARS-COV-2 is presented as follows

$$\frac{dS}{dt} = \Lambda - (\lambda + \mu)S, \tag{1a}$$

$$\frac{dE}{dt} = \lambda S - (\varepsilon + \theta + \mu)E, \tag{1b}$$

$$\frac{dA}{dt} = \varepsilon E - (\mu + \psi + \phi + \kappa)A, \tag{1c}$$

$$\frac{dI}{dt} = \theta E + \psi A - (\mu + \delta + \omega)I, \tag{1d}$$

$$\frac{dH}{dt} = \phi A + \omega I - (\mu + \delta + \rho)H, \tag{1e}$$

$$\frac{dR}{dt} = \kappa A + \rho H - \mu R, \tag{1f}$$

where

$$\lambda = \frac{\beta(I + \eta A)}{N}. \tag{2a}$$

The model is diagrammatically represented in Fig. 1, and the variables and parameters of the coronavirus model (1) are described in Tables 1 and 2, respectively.

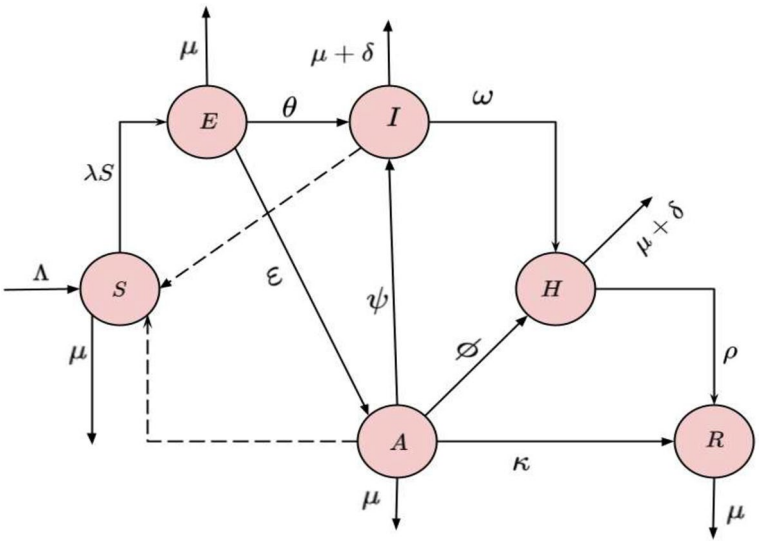

Fig. 1 Flow chart of the coronavirus model where λ is given in (1)

For computational convenience, we set

$$C_1 = (\varepsilon + \theta + \mu), \quad C_2 = (\mu + \psi + \phi + \kappa),$$
$$C_3 = (\mu + \delta + \omega), \quad C_4 = (\mu + \delta + \rho).$$

Then, the equations of the coronavirus model (1) become

$$\begin{aligned}
\frac{dS}{dt} &= \Lambda - (\lambda + \mu)S,\\
\frac{dE}{dt} &= \lambda S - C_1 E,\\
\frac{dA}{dt} &= \varepsilon E - C_2 A,\\
\frac{dI}{dt} &= \theta E + \psi A - C_3 I,\\
\frac{dH}{dt} &= \phi A + \omega I - C_4 H,\\
\frac{dR}{dt} &= \kappa A + \rho H - \mu R.
\end{aligned} \tag{3}$$

3 Basic properties of the model

The fundamental attributes exhibited by the coronavirus model (1) are carefully explored in this section.

3.1 Positivity of solutions

Here, it is noteworthy that every state variable and the associated epidemiological features describing the coronavirus model (1) are non-negative for all possible time $t > 0$ since the model explains the evolution of the coronavirus infection in the human population. Therefore, it is convenient to confirm that the parameters and variables of the coronavirus model (1) are non-negative for all times greater than zero.

Theorem 3.1 *The solutions* $S(t), E(t), A(t), I(t), H(t)$ and $R(t)$ *of the model* (1) *concerning the starting data* $S(0) > 0, E(0) > 0, A(0) > 0, I(0) > 0, H(0) > 0$ and $R(0) > 0$ *are all positive for all values of time greater than zero.*

Proof Let $t_1 = sup\{t > 0 : S(t) > 0, E(t) > 0, A(t) > 0, I(t) > 0, H(t) > 0 \text{ and } R(t) > 0\} > 0$, and recall that

$$\frac{dS}{dt} = \Lambda - (\lambda + \mu)S. \tag{4}$$

The following differential inequalities hold

$$\frac{dS}{dt} \geq -(\lambda + \mu)S \tag{5}$$

$$\int_0^{t_1} \frac{dS}{S(t)} \geq \int_0^{t_1} -(\lambda + \mu)dt \tag{6}$$

$$S(t_1) \geq S(0)e^{-\mu t_1 - \int_0^{t_1} \lambda(\tau)d\tau} \geq 0 \text{ as } t_1 \to \infty \tag{7}$$

Following the same process, it can be demonstrated that the other state variables are all greater than zero for all future values of t ($t > 0$), and hence, the verification ends here.

□

3.2 The Invariant region

Theorem 3.2 *Let* $S(t), E(t), A(t), I(t), H(t)$ and $R(t)$ *be the solutions of the coronavirus model* 1 *with the initial values* $S(0), E(0), A(0), I(0), H(0)$ and $R(0)$ *be positive for all values of* $t > 0$. *Then, the closed set*

$$D = \left\{ (S, E, A, I, H, R) \in R_+^6 : N \leq \frac{\Lambda}{\mu} \right\},$$

is positively invariant with non-negative initial values in R_+^6.

Proof The proof is done by adopting the procedures used in Ajao et al. (2023). Then, taking the summation of all the classes of (1) gives:

$$\frac{dN}{dt} = \Lambda - \mu N - \delta(I + H).$$

It then follows that

$$\frac{dN}{dt} \leq \Lambda - \mu N,$$

such that

$$N(t) \leq N(0)e^{-\mu t} + \frac{\Lambda}{\mu}(1 - e^{-\mu t})$$

If $N(0) \leq \frac{\Lambda}{\mu}$, then $N(t) \leq \frac{\Lambda}{\mu}$. Therefore, all solutions of the model with initial values in the biologically feasible region D stay in D for all $t > 0$. This implies that D is positively invariant. Thus, it suffices to explore the evolution of the coronavirus model (1) in the biologically feasible region D. □

4 Stability analysis

4.1 Disease-free equilibrium and the basic reproduction number

In a situation where Coronavirus does not exist in the community, the disease-free equilibrium is achieved which is represented by E_d^o and is given by

$$E_d^o = (S^0, E^0, A^0, I^0, H^0, R^0) = \left(\frac{\Lambda}{\mu}, 0, 0, 0, 0, 0\right) \tag{8}$$

The classical quantity, R_0, called the basic reproduction number is significant to the field of epidemiology as it determines the disease extinction and persistence in the society. The basic reproduction number is the average number of secondary COVID-19 cases caused by a coronavirus-infected person when introduced into a locality containing only the susceptible people van den Driessche and Watmough (2002). The basic reproduction number of the coronavirus model (1) is calculated based on the approach pointed out in van den Driessche and Watmough (2002). We define the new infection terms matrix F and the transition terms V as follows;

$$F = \begin{pmatrix} 0 & \beta\eta & \beta & 0 \\ 0 & 0 & 0 & 0 \\ 0 & 0 & 0 & 0 \\ 0 & 0 & 0 & 0 \end{pmatrix}, \tag{9}$$

and

$$V = \begin{pmatrix} c_1 & 0 & 0 & 0 & \\ -\varepsilon & C_2 & 0 & 0 & \\ -\theta & -\psi & C_3 & 0 & 0 \\ 0 & 0 & -\phi & w & 0 \\ 0 & 0 & -Z & 0 & T_5 \end{pmatrix}. \tag{10}$$

Then, $R_0 = \rho(FV^{-1})$, is given by

$$R_0 = \frac{\beta\,(\eta\,\varepsilon\,C_3 + \psi\,\varepsilon + \theta\,C_2)}{C_3 C_2 C_1} \tag{11}$$

The R_0 in (11) gives the average number of secondary infections that one COVID-19-infected individual can bring about when introduced in a community having only the susceptible individuals. Therefore, by using the Theorem 2 of Castillo-Chavez et al. (2002), the following result is claimed:

Lemma 4.1 *The disease-free equilibrium of the coronavirus model* (1) *is locally asymptotically stable whenever the associated basic reproduction number is less than unity* ($R_0 < 1$) *and otherwise if* $R_0 > 1$.

The epidemiological interpretation of lemma 4.1 is that COVID-19 can be wiped out from the locality if the sizes of starting subpopulations of the coronavirus model (1) are in the basin of attraction of E_d^o.

4.2 Endemic equilibrium

This section is dedicated to the investigation of the phenomenon where COVID-19 is prevalent in the population. If $E_1 = (S^*, E^*, A^*, I^*, H^*, R^*)$ is assigned to be the endemic equilibrium of the coronavirus model. Then, solving the model equations (1a)–(1f) simultaneously at steady state, gives

$$\begin{aligned}
S^* &= \frac{\pi}{\lambda^* + \mu}, \\
E^* &= \frac{\lambda^* \pi}{C_1(\lambda^* + \mu)}, \\
A^* &= \frac{\varepsilon \lambda^* \pi}{C_1 C_2(\lambda^* + \mu)}, \\
I^* &= \frac{(C_2\theta + \psi\varepsilon)\lambda^* \pi}{C_1 C_2 C_3(\lambda^* + \mu)}, \\
H^* &= \frac{[C_3\phi\varepsilon + \omega(C_2\theta + \psi\varepsilon)]\lambda^* \pi}{C_1 C_2 C_3 C_4(\lambda^* + \mu)}, \\
R^* &= \frac{\left[C_3 C_4 \kappa\varepsilon + \rho[C_3\phi\varepsilon + \omega(C_2\theta + \psi\varepsilon)]\right]\lambda^* \pi}{C_1 C_2 C_3 C_4(\lambda^* + \mu)}.
\end{aligned} \tag{12}$$

If the force of transmission (2a) associated with the endemic is assumed to be λ^*, then

$$\lambda^* = \frac{\beta(I^* + \eta A^*)}{N^*}. \tag{13}$$

Substituting (12) into (13) leads to

$$P_1\lambda^{*2} + P_2\lambda^* + P_3 = 0, \tag{14}$$

where

$$\begin{aligned} P_1 = {} & C_2C_3C_4\mu + C_3C_4\varepsilon\mu + C_4\mu(C_2\theta + \psi\varepsilon) + \mu\left[C_3\phi\varepsilon + \omega(C_2\theta + \psi\varepsilon)\right] \\ & + \left[C_3C_4\kappa\varepsilon + \rho[C_3\phi\varepsilon + \omega(C_2\theta + \psi\varepsilon)]\right], \end{aligned} \tag{15}$$

$$P_2 = \mu[P_1 + (1 - R_0)C_1C_2C_3C_4], , \tag{16}$$

$$P_3 = (1 - R_0)C_1C_2C_3C_4\mu^2. \tag{17}$$

From (14), $P_1 > 0$, $P_3 > 0$ if $R_0 < 1$ and $P_3 < 0$ if $R_0 > 1$. Therefore, the following result is obtained:

Theorem 4.1 *The COVID-19 model (1) has*

1. *a unique endemic equilibrium if* $P_3 < 0$ (*Corresponding to when* $R_0 > 1$)
2. *a unique endemic equilibrium if* $P_2 < 0$ *and* $P_3 = 0$ *or* $P_2^2 - 4P_1P_3 = 0$
3. *two endemic equilibria if* $P_3 > 0$ *and* $P_2 < 0$ *or* $P_2^2 - 4P_1P_3 > 0$
4. *none otherwise*

This indicates that multiple equilibria will exist when the reproduction number (R_0) is less than unity

4.3 Global stability of endemic equilibrium: special case

The behaviour of the transmission dynamics of the coronavirus model (1) around the endemic equilibrium point, E_1^*, is examined specifically when $\theta = \phi = 0$, and $\delta = 0$, which translates to the absence of progression rate from $E(t)$ to I(t), hospitalized rate, and COVID-19-associated death rate. Then, the coronavirus model has the endemic equilibrium as

$$E_1^* = (S^{**}, E^{**}, A^{**}, I^{**}, H^{**}, R^{**}). \tag{18}$$

By assuming $\delta = 0$, thus $N \to \frac{\Lambda}{\mu}$ as $t \to \infty$ and by so doing, the force of infection reduces to

$$\lambda = \hat{\beta}(I + \eta A), \tag{19}$$

where

$$\hat{\beta} = \frac{\beta\mu}{\Lambda}.$$

Furthermore, let the associated basic reproduction number of the model when $\theta = \phi = \delta = 0$ be $\hat{R_0} = R_{0|\theta=\phi=\delta=0}$.

Theorem 4.2 *Consider the COVID-19 model (1) when $\theta = \phi = 0$. The endemic equilibrium, E_1^*, of the coronavirus model (1) is globally asymptotically stable in $D\backslash D_o$ whenever $\hat{R}_0 > 1$, where*

$$D_o = \{(S, E, A, I, H, R) \in D : E = A = I = H = R = 0\}.$$

Proof Consider the COVID-19 model (1) having $\theta = \phi = 0$ with (19) and $\hat{R}_0 > 1$, we use the Lyapunov function given by

$$\begin{aligned} L =& S - S^{**} - S^{**} ln\frac{S}{S^{**}} + E - E^{**} - E^{**} ln\frac{E}{E^{**}} + X\left[A - A^{**} - A^{**} ln\frac{A}{A^{**}}\right] \\ &+ Y\left[I - I^{**} - I^{**} ln\frac{I}{I^{**}}\right] + Z\left[H - H^{**} - H^{**} ln\frac{H}{H^{**}}\right]. \end{aligned} \tag{20}$$

Taking the time derivative of (20) leads to

$$\begin{aligned} L' =& S' - \frac{S^{**}}{S}S' + E' - \frac{E^{**}}{E}E' + X\left[A' - \frac{A^{**}}{A}A'\right] + Y\left[I' - \frac{I^{**}}{I}I'\right] \\ &+ Z\left[H' - \frac{H^{**}}{H}H'\right], \end{aligned} \tag{21}$$

where

$$X = \frac{C_1}{\varepsilon}, \tag{22}$$

$$Y = \frac{C_1 C_2 - \hat{\beta} S \eta \varepsilon}{\varepsilon \psi}, \tag{23}$$

$$Z = \frac{C_1 C_2 C_3 - \hat{\beta} S \eta \varepsilon C_3 - \hat{\beta} S \varepsilon \psi}{\varepsilon \omega \psi}, \tag{24}$$

with $\Lambda = \hat{\beta}(I^{**} + \eta A^{**})S^{**} + \mu S^{**}$, Equation (21) becomes

$$\begin{aligned} L' =& \mu S^{**} - \mu S + \hat{\beta}(I^{**} + \eta A^{**})S^{**} \\ &- \left[\frac{\mu S^{**2} - \mu S^{**} + \hat{\beta}(I^{**} + \eta A^{**})S^{**2}}{S} - \hat{\beta}(I^{**} + \eta A^{**})S^{**}\right] \\ &- C_1 E - \frac{\hat{\beta}(I + \eta A)SE^{**}}{E} + C_1 E^{**} + \frac{C_1}{\varepsilon}\left[\varepsilon E - C_2 A - \frac{\varepsilon E A^{**}}{A} + C_2 A^{**}\right] \\ &+ \frac{C_1 C_2 - \hat{\beta} S \eta \varepsilon}{\varepsilon \psi}\left[\psi A - C_3 - \frac{\psi A I^{**}}{I} + C_3 I^{**}\right] + \frac{C_1 C_2 C_3 - \hat{\beta} S \eta \varepsilon C_3 - \hat{\beta} S \varepsilon \psi}{\varepsilon \omega \psi} \\ &\times \left[\omega I - C_4 H - \frac{\omega I H^{**}}{H} + C_4 H\right]. \end{aligned} \tag{25}$$

Further simplification with

$$C_1 = \frac{\hat{\beta}(I^{**} + \eta A^{**})S^{**}}{E^{**}}, \qquad C_2 = \frac{\varepsilon E^{**}}{A^{**}}, \qquad C_3 = \frac{\psi A^{**}}{I^{**}}, \qquad C_4 = \frac{\omega I^{**}}{H^{**}}, \tag{26}$$

leads to

$$L' = \mu S^{**} - \mu S + 3\hat{\beta}(I^{**} + \eta A^{**})S^{**} + \hat{\beta} I^{**} S^{**} - \frac{\hat{\beta}(I^{**} + \eta A^{**})S^{**2}}{S} - \frac{\mu S^{**2}}{S} + \mu S^{**} - \frac{\hat{\beta}(I + \eta A)SE^{**}}{E} - \frac{\hat{\beta}(I^{**} + \eta A^{**})S^{**}EA^{**}}{E^{**}A} - \frac{\hat{\beta} I^{*2} A S^{**}}{A^{**} I}. \tag{27}$$

Then, it follows that

$$L' = \hat{\beta} I^{**} S^{**}\left(4 - \frac{S^{**}}{S} - \frac{AI^{**}}{A^{**}I} - \frac{EA^{**}}{E^{**}A} - \frac{SIE^{**}}{S^{**}I^{**}E}\right) + \mu S^{**}\left(2 - \frac{S^{**}}{S} - \frac{S}{S^{**}}\right) + \hat{\beta}\eta A^{**} S^{**}\left(3 - \frac{S^{**}}{S} - \frac{SAE^{**}}{S^{**}A^{**}E} - \frac{EA^{**}}{E^{**}A}\right). \tag{28}$$

Therefore, with the A.M surpassing G.M, the following inequalities hold:

$$2 - \frac{S^{**}}{S} - \frac{S}{S^{**}} \leq 0, \quad 4 - \frac{S^{**}}{S} - \frac{SIE^{**}}{S^{**}I^{**}E} - \frac{EA^{**}}{E^{**}A} - \frac{AI^{**}}{A^{**}I} \leq 0, \quad 3 - \frac{S^{**}}{S} - \frac{SAE^{**}}{S^{**}A^{**}E} - \frac{EA^{**}}{E^{**}A} \leq 0.$$

Therefore, $L' \leq 0$ for $\hat{R}_0 > 1$. Thus, L is a Lyapunov function in $D \backslash D_o$, and on the basis of LaSalle's Invariance Principle LaSalle (1976), all trajectories of the coronavirus model with the starting conditions in $D \backslash D_o$ go to the associated endemic equilibrium E_1^* as $t \to \infty$ whenever $\hat{R}_0 > 1$. This, therefore, terminates the proof. □

As a consequence, the implication of the global asymptotic stability of E_1^* demonstrated in Theorem (4.3) from the biological viewpoint is that the coronavirus disease will be prevalent in the locality whenever the associated basic reproduction number transcends unity, however large or however small the initial populations of the model. This result is corroborated by quantitative illustrations displayed in Figs. 2, 3 and 4.

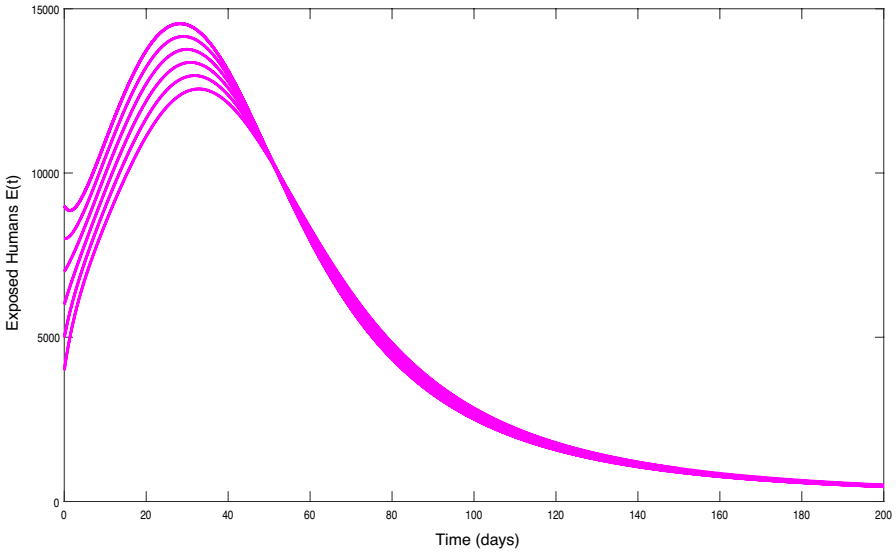

Fig. 2 Convergence of the solutions of the exposed population to the endemic equilibrium regardless of the values of initial conditions, using the parameter values presented in Table 3 except for $\beta = 0.7$

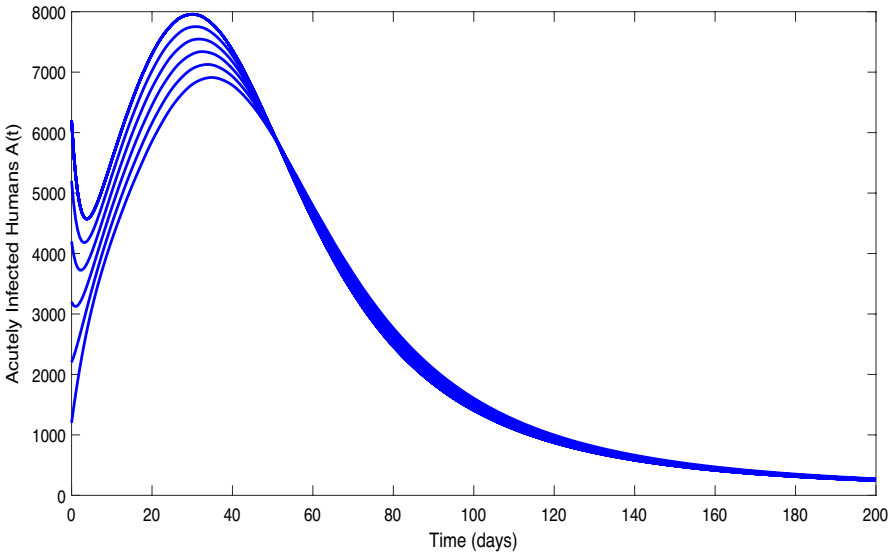

Fig. 3 Convergence of the acutely-infected population to the endemic equilibrium regardless of the values of initial conditions, using the parameter values presented in Table 3 except for $\beta = 0.7$

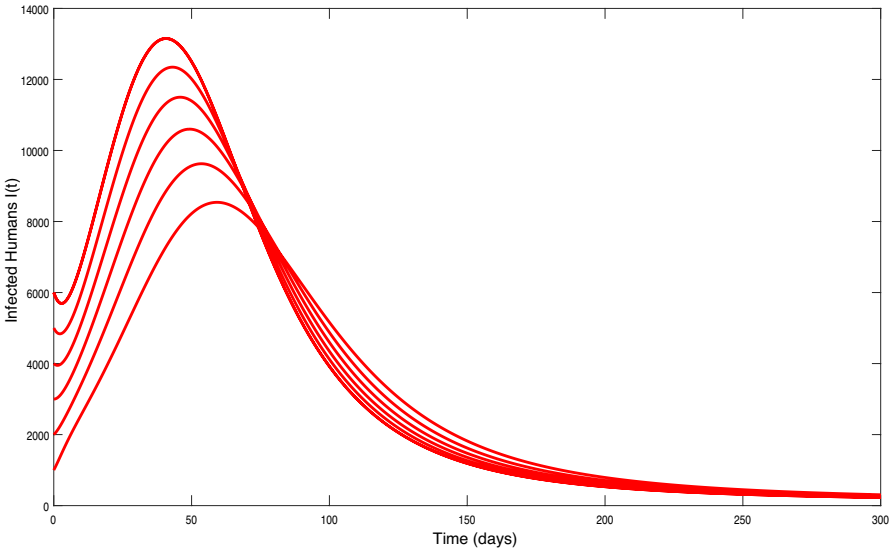

Fig. 4 Convergence of infectious population trajectories to the endemic equilibrium regardless of the values of initial conditions, using the parameter values presented in Table 3 except for $\beta = 0.7$

5 Sensitivity analysis

This section examines the behaviour of certain important epidemiological features of the model on the dynamics of the deadly coronavirus infection. As a result, the influence of

Table 3 Values of the parameters used in model 1

Parameter	Baseline value	Range	Source
β	0.492	0.002−0.75	Garba et al. (2020)
η	0.4	0–1	Assumed
μ	0.01277	0.0107−0.0148	Oke et al. (2023)
ε	0.18	0.098−0.278	Cauchemez et al. (2014)
θ	0.02	0.009−0.4	Assumed
ψ	0.1	0.05−0.5	Kouidere et al. (2023)
δ	0.036	0.01−0.06	Garba et al. (2020)
Λ	1500	500-3500	Yang et al. (2022)
ρ	0.096	0.0625−0.125	Ferguson et al. (2020)
ω	0.0264	0.0059−0.0679	Okuonghae and Omame (2020)
ϕ	0.083	0.04−0.2	Paul et al. (2023)
κ	0.13978	0.033−0.333	Tang et al. (2020)

Table 4 Sensitivity analysis result

Parameter	PRCC value	Parameter	PRCC value
β	0.9614	η	0.1439
μ	−0.0610	ε	−0.1566
θ	0.5005	ψ	0.3626
ω	−0.7102	ϕ	−0.1504
κ	−0.2047	δ	−0.6221

each parameter of the coronavirus model associated with the basic reproduction number ($\mathcal{R}_0$) is painstakingly audited through sensitivity analysis.

At this juncture, it is imperative to state that the consequence of the sensitivity analysis enables predictions for efficient control measures to be considered in mitigating the coronavirus invasion in the population. One of the ways to achieve this is by conducting the sensitivity analysis of such a model with the help of the normalized forward sensitivity index as pointed out in Olaniyi and Obabiyi (2014), Kifle and Obsu (2022), Paul and Kuddus (2022). The definition of the normalized forward sensitivity index of the basic reproduction number, $\mathcal{R}_0$, that depends differentiably on a parameter, $\mathbf{b}$, is given as

$$\Upsilon_{\mathbf{b}}^{\mathcal{R}_0} = \frac{\partial \mathcal{R}_0}{\partial \mathbf{b}} \left(\frac{\mathbf{b}}{\mathcal{R}_0} \right). \tag{29}$$

Consequently, the sensitivity analysis of the parameters relative to the threshold quantity, $\mathcal{R}_0$, is examined using the values specified in Table 3 and results are summarised in Table 4. It is instructive to state that Latin Hypercube Sampling or Partial Rank Correlation Coefficient (LHS/PRCC), a more realistic and robust aspect of sensitivity analysis involving several parameter spaces is adopted to corroborate the sensitivity analysis as presented in Table 3. It is noticed in Fig. 5 that the transmission rate, β, modification parameter, η, movement rates, ψ, and θ have positive PRCCs implying that these COVID-19 model

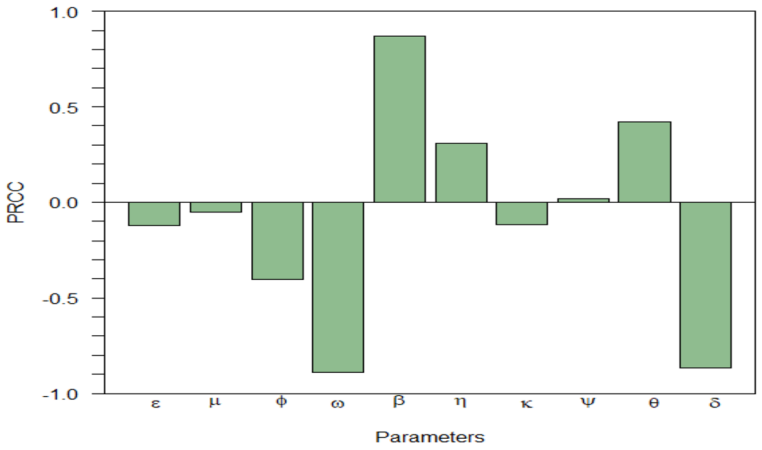

Fig. 5 PRCC chart of different parameters when R_0 serves as the response function

parameters are positively correlated to the basic reproduction number. Any shoot-up in these parameter values tends to elevate the basic reproduction number indicating the endemicity of SARS-CoV-2 in the community. It should be noted that the positive correlation of β to $\mathcal{R}_0$ suggests that efforts should be intensified on measures that will effectively downsize the infection rate of COVID-19 in a susceptible environment. This, therefore, encourages the optimum use of non-pharmaceutical interventions to set the dynamics spread of the disease to total extinction. In a similar spirit, the positive correlation of the modification parameter η suggests that control measures that will mitigate the degree of infectiousness of an acutely infected individual should be enforced. Additionally, the implication of the positive correlation of the parameters θ and ϕ is that COVID-19 will be prevalent if efforts are not sought early enough to curb the progression of COVID-19.

Furthermore, it is also noted that parameters such as ε representing movement rate, natural mortality rate, μ, ϕ and ω, describing hospitalization rate of acutely infected and infectious individuals, recovery rate, κ, and coronavirus mortality rate, δ have negative correlation coefficients with regard to the basic reproduction number. Thus, any slight increment in these parameter values will downplay the basic reproduction number's value. The implication of this from the perspective of epidemiology is that coronavirus elimination from the population is guaranteed if serious attention can be given to the parameters that lower the COVID-19 reproduction number.

6 Optimal control model

This section introduces the optimal control version of our proposed model based on the results of the sensitivity analysis carried out in section 5. Specifically, the transmission rate of COVID-19, β, the modification (infectivity) parameter for the acutely infected individuals, η, and the movement rate from E class to I class have impacts on the spread of the coronavirus. To reduce the intensity of these parameters, we introduced

the following time-dependent controls: public education, $u_1(t)$, vaccination with a single dose, $u_2(t)$, vaccination with the second dose, $u_3(t)$, an increase in polymerase chain reaction (PRC) testing equipment, $u_4(t)$, hospitalization rate $u_5(t)$, and treatment rate (prophylaxis) $u_6(t)$. Furthermore, the parameters that significantly lessen the infection burden in the proposed model are the COVID-19-related death rate, δ, and the hospitalization rates of acutely infected and infectious persons, ϕ and ω, respectively. But it is logical that at every event of disease spread, the rate of preventing people from dying is a major concern to society, so the disease-induced death rate cannot be used as a control measure. Therefore, we additionally impose time-dependent controls on ϕ and ω, denoted as detection rate and availability of hospital beds, $u_5(t)$. Hence, the modified version of the COVID-19 model 1 with time-dependent optimal controls is given as

$$\begin{aligned}
\frac{dS}{dt} &= \Lambda - \left(\frac{(1-u_1(t)-u_2(t)-u_3(t))\beta(I+\eta A)}{S+E+A+I+H+R} + \mu\right)S,\\
\frac{dE}{dt} &= \frac{(1-u_1(t)-u_2(t)-u_3(t))\beta(I+\eta A)S}{S+E+A+I+H+R} - (\varepsilon + (1-u_4(t)) + \mu)E,\\
\frac{dA}{dt} &= \varepsilon E - (\mu + u_5(t) + \kappa)A,\\
\frac{dI}{dt} &= (1-u_4(t))E + \psi A - (\mu + \delta + u_5(t))I,\\
\frac{dH}{dt} &= u_5(t)A + u_5(t)I - (\mu + \delta + u_6(t))H,\\
\frac{dR}{dt} &= \kappa A + u_6(t)H - \mu R.
\end{aligned}$$

Further, our main goal is to lessen the subpopulations of exposed, acutely infected, infectious and increase hospitalization and polymerase chain reaction (PRC) testing equipment, and the cost reduction of controls implementation so that the objective or cost functional, denoted as J, is given by

$$J(u_1,u_2,u_3,u_4,u_5,u_6) = \int_0^{t_f} \left(T_1E + T_2A + T_3I + T_4H + \frac{1}{2}K_1u_1^2 + \frac{1}{2}K_2u_2^2 + \frac{1}{2}K_3u_3^2 + \frac{1}{2}K_4u_4^2 + \frac{1}{2}K_5u_5^2 + \frac{1}{2}K_6u_6^2\right)dt. \tag{30}$$

In (30), T_1, T_2, T_3 and T_4 are the positive balancing weight constants for exposed, acutely infected individuals, infectious individuals, and hospitalized infected individuals, respectively. For instance, choosing T_1 greater than T_2, T_3 and T_4 suggests that control is more focused on decreasing the exposed humans than decreasing the numbers of acutely infected persons, infectious, and hospitalized humans. The terms $\frac{1}{2}K_1u_1^2$, $\frac{1}{2}K_2u_2^2$, $\frac{1}{2}K_3u_3^2$, $\frac{1}{2}K_4u_4^2$, $\frac{1}{2}K_5u_5^2$, $\frac{1}{2}K_6u_6^2$ describe the costs in the reduction of the disease in each class, respectively. Whereas t_f is the terminal time expected to implement the control intervention strategies. To show the nonlinearity of the costs of implementation, we use the standard quadratic functional as in other previous works (for example, see Asamoah et al. 2020, 2022, Asamoah et al. 2021, Asamoah et al. 2021, 2023 and some of the references cited therein). Our aim is to obtain the optimal control $u^* = (u_i^*)$, $(i = 1,2,3,4,5,6)$, such that

$$J(u^*) = \min\{J(u_i) : u_i \in U\}, \tag{31}$$

where U represent a set of Lebesgue measurable control given by

$$U = \{u_i : 0 \leq u_{imin} \leq u_i(t) \leq u_{imax} \leq 1,\ 0 \leq t \leq t_f\}.$$

Using the existence results as pointed out in Fleming and Richel (2012) coupled with the explicit approach x-rayed in Abidemi et al. (2022), Olaniyi et al. (2023), we show the existence of an optimal control which satisfies problem (31), with regard to the time-variant COVID-19 system (30).

6.1 Control characterization

The optimal control problem (31) with regard to the optimal control model (30) is changed to a problem of minimizing pointwise a Hamiltonian H, with the help of the celebrated Pontryagin's maximum principle Pontryagin et al. (1962). The Hamiltonian, $\mathcal{H}$ function is defined by

$$\begin{aligned} HDD =& \lambda_R \left(H u_6 + A\kappa - R\mu\right) - \lambda_I \left(\mathrm{I}\left(u_5 + \delta + \mu\right) - A\psi + \mathrm{E}\left(u_4 - 1\right)\right) \\ &+ \frac{K_1 {u_1}^2}{2} + \frac{K_2 {u_2}^2}{2} + \frac{K_3 {u_3}^2}{2} + \frac{K_4 {u_4}^2}{2} + \frac{K_5 {u_5}^2}{2} + \frac{K_6 {u_6}^2}{2} \\ &- \lambda_E \left(\mathrm{E}\left(-u_4 + \varepsilon + \mu + 1\right) + \frac{\beta\left(A\eta + \mathrm{I}\right)\left(u_1 + u_2 + u_3 - 1\right)S}{S + A + \mathrm{E} + H + \mathrm{I} + R}\right) + \lambda_A \left(\mathrm{E}\,\varepsilon - A\left(u_5 + \kappa + \mu\right)\right) \\ &+ \lambda_S \left(\Lambda - S\left(\mu - \frac{\beta\left(A\eta + \mathrm{I}\right)\left(u_1 + u_2 + u_3 - 1\right)}{S + A + \mathrm{E} + H + \mathrm{I} + R}\right)\right) + \lambda_H \left(A u_5 + \mathrm{I} u_5 - H\left(u_6 + \delta + \mu\right)\right) \\ &+ A T_2 + \mathrm{E} T_1 + H T_4 + \mathrm{I} T_3, \end{aligned} \tag{32}$$

where $_n, n = S, A, E, I, H, R$, are the corresponding adjoint variables to the state variables $S, E, A, I, H,$ and$R$, of the optimal control model (30). The required costate variables conditions and characterization of the six controls for the optimal control problem are established in the next result.

Theorem 6.1 *Considering an optimal control u^* in a way that $J(u^*) = \min\{J(u_i) : u_i \in U\}$, then there exist costate variables $_n$ satisfying the adjoint system*

$$\begin{aligned}
\frac{d\lambda_S}{dt} &= -diff(HDD, S),\\
&= \lambda_S\left(\mu - \frac{\beta(A\eta+\mathrm{I})\left(u_1+u_2+u_3-1\right)}{S+A+\mathrm{E}+H+\mathrm{I}+R} + \frac{S\beta(A\eta+\mathrm{I})\left(u_1+u_2+u_3-1\right)}{(S+A+\mathrm{E}+H+\mathrm{I}+R)^2}\right)\\
&\quad + \frac{\beta\lambda_E(A\eta+\mathrm{I})\left(u_1+u_2+u_3-1\right)}{(S+A+\mathrm{E}+H+\mathrm{I}+R)} - \frac{\beta\lambda_E(A\eta+\mathrm{I})\left(u_1+u_2+u_3-1\right)}{(S+A+\mathrm{E}+H+\mathrm{I}+R)^2},\\
\frac{d\lambda_E}{dt} &= -diff(HDD, E),\\
&= \lambda_E\left(\mu - u_4 + \varepsilon - \frac{\beta(A\eta+\mathrm{I})\left(u_1+u_2+u_3-1\right)S}{(S+A+\mathrm{E}+H+\mathrm{I}+R)^2} + 1\right)\\
&\quad -\lambda_A\varepsilon - T_1 + \lambda_I\left(u_4-1\right) + \frac{S\beta\lambda_S(A\eta+\mathrm{I})\left(u_1+u_2+u_3-1\right)}{(S+A+\mathrm{E}+H+\mathrm{I}+R)^2},\\
\frac{d\lambda_A}{dt} &= -diff(HDD, A),\\
&= \lambda_E\left(\frac{\beta\eta\left(u_1+u_2+u_3-1\right)S}{S+A+\mathrm{E}+H+\mathrm{I}+R} - \frac{\beta(A\eta+\mathrm{I})\left(u_1+u_2+u_3-1\right)S}{(S+A+\mathrm{E}+H+\mathrm{I}+R)^2}\right)\\
&\quad -\kappa\lambda_R - T_2 - \lambda_I\psi - \lambda_H u_5 + \lambda_A\left(u_5+\kappa+\mu\right)\\
&\quad -S\lambda_S\left(\frac{\beta\eta\left(u_1+u_2+u_3-1\right)}{S+A+\mathrm{E}+H+\mathrm{I}+R} - \frac{\beta(A\eta+\mathrm{I})\left(u_1+u_2+u_3-1\right)}{(S+A+\mathrm{E}+H+\mathrm{I}+R)^2}\right),\\
\frac{d\lambda_I}{dt} &= -diff(HDD, I),\\
&= \lambda_I\left(u_5+\delta+\mu\right) - \lambda_H u_5 - T_3\\
&\quad +\lambda_E\left(\frac{\beta\left(u_1+u_2+u_3-1\right)S}{S+A+\mathrm{E}+H+\mathrm{I}+R} - \frac{\beta(A\eta+\mathrm{I})\left(u_1+u_2+u_3-1\right)S}{(S+A+\mathrm{E}+H+\mathrm{I}+R)^2}\right)\\
&\quad -S\lambda_S\left(\frac{\beta\left(u_1+u_2+u_3-1\right)}{S+A+\mathrm{E}+H+\mathrm{I}+R} - \frac{\beta(A\eta+\mathrm{I})\left(u_1+u_2+u_3-1\right)}{(S+A+\mathrm{E}+H+\mathrm{I}+R)^2}\right),\\
\frac{d\lambda_H}{dt} &= -diff(HDD, H),\\
&= \lambda_H\left(u_6+\delta+\mu\right) - \lambda_R u_6 - T_4 - \frac{\beta\lambda_E(A\eta+\mathrm{I})\left(u_1+u_2+u_3-1\right)S}{(S+A+\mathrm{E}+H+\mathrm{I}+R)^2}\\
&\quad + \frac{S\beta\lambda_S(A\eta+\mathrm{I})\left(u_1+u_2+u_3-1\right)}{(S+A+\mathrm{E}+H+\mathrm{I}+R)^2},\\
\frac{d\lambda_R}{dt} &= -diff(HDD, R),\\
&= \lambda_R\mu - \frac{\beta\lambda_E(A\eta+\mathrm{I})\left(u_1+u_2+u_3-1\right)S}{(S+A+\mathrm{E}+H+\mathrm{I}+R)^2} + \frac{S\beta\lambda_S(A\eta+\mathrm{I})\left(u_1+u_2+u_3-1\right)}{(S+A+\mathrm{E}+H+\mathrm{I}+R)^2}.
\end{aligned}$$

with transversality conditions

$$\lambda_n(t_f) = 0,\ n = S, A, E, I, H, R, \tag{33}$$

and optimal control characterizations

$$\begin{aligned}
u_1^* &= \frac{\frac{S\beta\lambda_E(A\eta+\mathrm{I})}{S+A+\mathrm{E}+H+\mathrm{I}+R} - \frac{S\beta\lambda_S(A\eta+\mathrm{I})}{S+A+\mathrm{E}+H+\mathrm{I}+R}}{K_1},\\
u_2^* &= \frac{\frac{S\beta\lambda_E(A\eta+\mathrm{I})}{S+A+\mathrm{E}+H+\mathrm{I}+R} - \frac{S\beta\lambda_S(A\eta+\mathrm{I})}{S+A+\mathrm{E}+H+\mathrm{I}+R}}{K_2},\\
u_3^* &= \frac{\frac{S\beta\lambda_E(A\eta+\mathrm{I})}{S+A+\mathrm{E}+H+\mathrm{I}+R} - \frac{S\beta\lambda_S(A\eta+\mathrm{I})}{S+A+\mathrm{E}+H+\mathrm{I}+R}}{K_3},\\
u_4^* &= -\frac{\mathrm{E}\lambda_E - \mathrm{E}\lambda_I}{K_4},\\
u_5^* &= \frac{A\lambda_A + \mathrm{I}\lambda_I - \lambda_H(A+\mathrm{I})}{K_5},\\
u_6^* &= \frac{H\lambda_H - H\lambda_R}{K_6}.
\end{aligned} \tag{34}$$

Proof The proof is premised on finding the partial derivatives of the Hamiltonian, $\mathcal{H}$, with regard to all of the state variables S, E, A, I, H and R, respectively, as defined hereunder

$$\frac{d\lambda_n}{dt} = -\left(\frac{\partial\mathcal{H}}{\partial n}\right),\ \ \lambda_n(t_f) = 0,\ \ with\ \ n = S, E, A, I, H, R. \tag{35}$$

In addition, the optimal control characterization is obtained through the implementation of the following optimality condition and by finding the solutions of the controls $u_i, i = 1, 2, 3, 4, 5, 6$.

$$\begin{aligned}
du_1 &= diff(HDD, u_1)\\
&= K_1 u_1 - \frac{S\beta\lambda_E(A\eta+\mathrm{I})}{S+A+\mathrm{E}+H+\mathrm{I}+R} + \frac{S\beta\lambda_S(A\eta+\mathrm{I})}{S+A+\mathrm{E}+H+\mathrm{I}+R},
\end{aligned} \tag{36}$$

$$\begin{aligned}
du_2 &= diff(HDD, u_2)\\
&= K_2 u_2 - \frac{S\beta\lambda_E(A\eta+\mathrm{I})}{S+A+\mathrm{E}+H+\mathrm{I}+R} + \frac{S\beta\lambda_S(A\eta+\mathrm{I})}{S+A+\mathrm{E}+H+\mathrm{I}+R},
\end{aligned} \tag{37}$$

$$\begin{aligned}
du_3 &= diff(HDD, u_3)\\
&= K_3 u_3 - \frac{S\beta\lambda_E(A\eta+\mathrm{I})}{S+A+\mathrm{E}+H+\mathrm{I}+R} + \frac{S\beta\lambda_S(A\eta+\mathrm{I})}{S+A+\mathrm{E}+H+\mathrm{I}+R},
\end{aligned} \tag{38}$$

$$\begin{aligned}
du_4 &= diff(HDD, u_4)\\
&= K_4 u_4 + \mathrm{E}\lambda_E - \mathrm{E}\lambda_I,
\end{aligned} \tag{39}$$

$$\begin{aligned}
du_5 &= diff(HDD, u_5)\\
&= K_5 u_5 - \mathrm{I}\lambda_I - A\lambda_A + \lambda_H(A+\mathrm{I}),
\end{aligned} \tag{40}$$

$$\begin{aligned}
du_6 &= diff(HDD, u_6)\\
&= K_6 u_6 - H\lambda_H + H\lambda_R.
\end{aligned} \tag{41}$$

Now, by adopting the standard bounds for the controls $u_i(t)$, $(i = 1, 2, 3, 4)$ yields

$$u_i(t)^* = \begin{cases} u_i, \text{ if } 0 \le u_i \le 1, \\ 0, \text{ if } u_i \le 0, \\ 1, \text{ if } u_i \ge 1, \end{cases} \tag{42}$$

where

$$u_1 = \frac{\frac{S\beta\,\lambda_E\,(A\,\eta+\mathrm{I})}{S+A+\mathrm{E}+H+\mathrm{I}+R} - \frac{S\,\beta\,\lambda_S\,(A\,\eta+\mathrm{I})}{S+A+\mathrm{E}+H+\mathrm{I}+R}}{K_1},$$

$$u_2 = \frac{\frac{S\beta\,\lambda_E\,(A\,\eta+\mathrm{I})}{S+A+\mathrm{E}+H+\mathrm{I}+R} - \frac{S\,\beta\,\lambda_S\,(A\,\eta+\mathrm{I})}{S+A+\mathrm{E}+H+\mathrm{I}+R}}{K_2},$$

$$u_3 = \frac{\frac{S\beta\,\lambda_E\,(A\,\eta+\mathrm{I})}{S+A+\mathrm{E}+H+\mathrm{I}+R} - \frac{S\,\beta\,\lambda_S\,(A\,\eta+\mathrm{I})}{S+A+\mathrm{E}+H+\mathrm{I}+R}}{K_3},$$

$$u_4 = -\frac{\mathrm{E}\,\lambda_E - \mathrm{E}\,\lambda_I}{K_4},$$

$$u_5 = \frac{A\,\lambda_A + \mathrm{I}\,\lambda_I - \lambda_H\,(A+\mathrm{I})}{K_5},$$

$$u_6 = \frac{H\,\lambda_H - H\,\lambda_R}{K_6}.$$

□

6.2 Effect of parameters of the COVID-19 model

Herein, the effect of the transmission rate of COVID-19 on the exposed population, COVID-19-acutely infected humans and infectious humans, respectively, are demonstrated in Fig. 6. It is observed that an increase in the COVID-19 transmission rate from an infected individual leads to a corresponding increase in the populations of $E(t), A(t)$and.$I(t)$. This implies that a surge in the effective contact of susceptible individuals with COVID-19 infected individuals will result in the prevalence of the disease in the population when there are no effective controls or preventive measures set in place to nip the disease dynamics into the bud. From another perspective, Fig. 7 flaunts how the transmission rate, β, of COVID-19 and the modification parameter, η, measuring the degree of infectiousness of acutely infected humans affect the basic reproduction number. An increase in any of these parameters is noticed to accelerate the prevalence of coronavirus disease in the population.

6.3 Simulations of the optimality system

The optimality system which is a combination of the state equation (30) with the co-state equation (33) and the optimal control characterizations (34) in conjunction with the initial sizes and corresponding transversality conditions are numerically solved with the help of forward-backward Runge–Kutta method of order four, implemented in MatLab. The forward-backward solution approach is used following the procedures x-rayed in Akanni

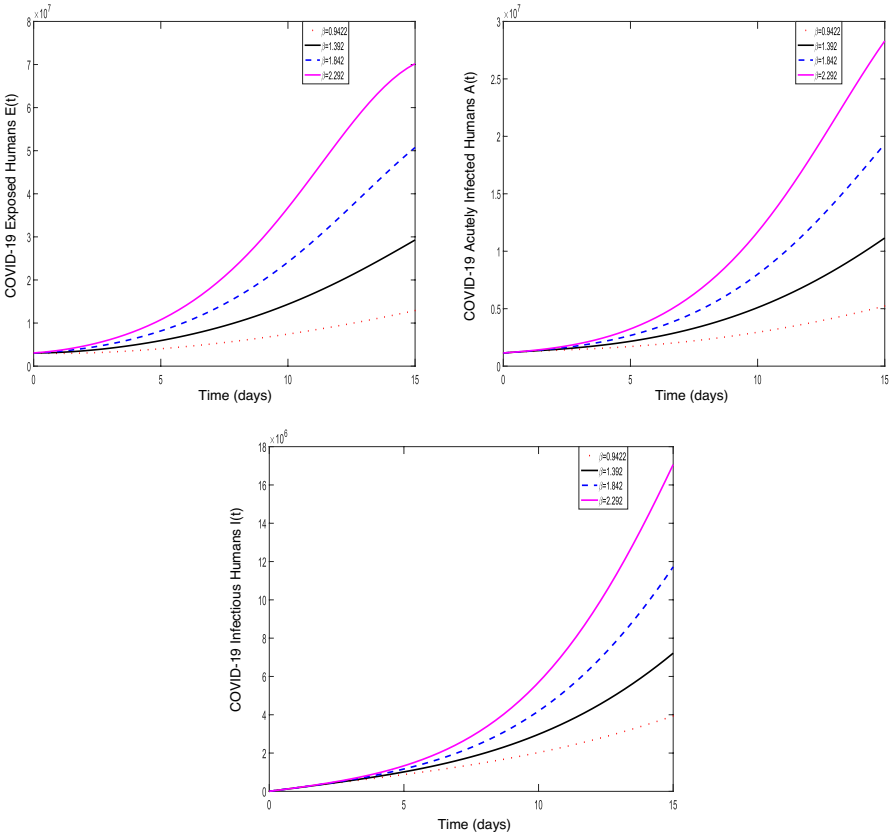

Fig. 6 Effect of transmission probability, β, on the subpopulations

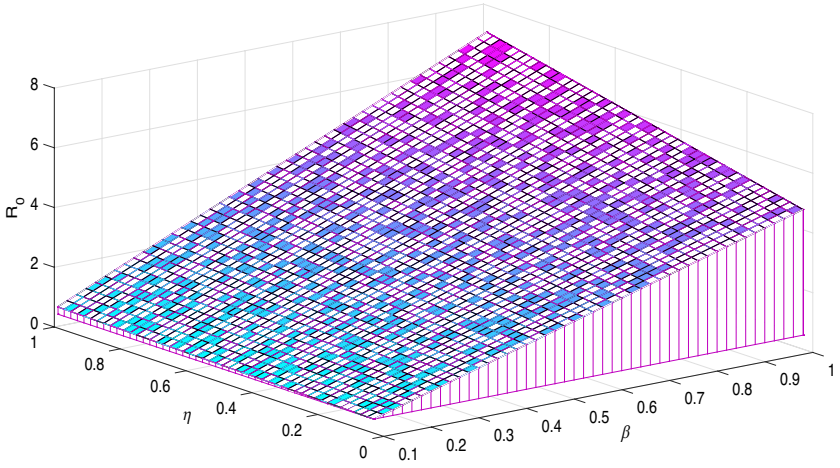

Fig. 7 3-D plot showcasing the effects of modification parameter for infectiousness of acutely infected humans and transmission rate on the basic reproduction number of the COVID-19 model

et al. (2020), Khan et al. (2022), Olaniyi et al. (2020), Sharma and Samanta (2015). Utilizing the parameter values presented in Table3, the numerical experiments of the optimality system are executed over a time frame [0, 15], implying that the terminal time for interventions' execution is chosen as $t_f = 15$ weeks. While the starting sizes of the state variables are taken as $S(0) = 268850000$, $E(0) = 3065400$, $A(0) = 1146200$, $I(0) = 4085$, $H(0) = 136$, $R = 416600$. The balancing weight and rate constants of the functional J are, respectively, taken as $T_1 = 800$, $T_2 = 900$, $T_3 = 750$, $T_4 = 900$, $K_1 = 5$, $K_2 = 7$, $K_3 = 9$, $K_4 = 70$, $K_5 = 60$ and $K_6 = 800$. The influence of six distinct scenarios, combining any two or more time-dependent controls on the population of exposed, acutely infected, and infectious humans are explored in Figs. 8, 9, 10, 11, 12, 13. The intervention scenarios considered are listed as follows:

(i) Scenario **A**: combination of $u_1(t)$ and $u_3(t)$,
(ii) Scenario **B**: combination of $u_1(t)$ and $u_4(t)$,
(iii) Scenario **C**: combination of $u_2(t)$ and $u_3(t)$,
(iv) Scenario **D**: combination of $u_1(t)$, $u_2(t)$ and $u_3(t)$,
(v) Scenario **E**: combination of $u_2(t)$, $u_3(t)$ and $u_6(t)$,
(vi) Scenario **F**: combination of $u_1(t), u_2(t), u_3(t), u_4(t), u_5(t)$ and $u_6(t)$.

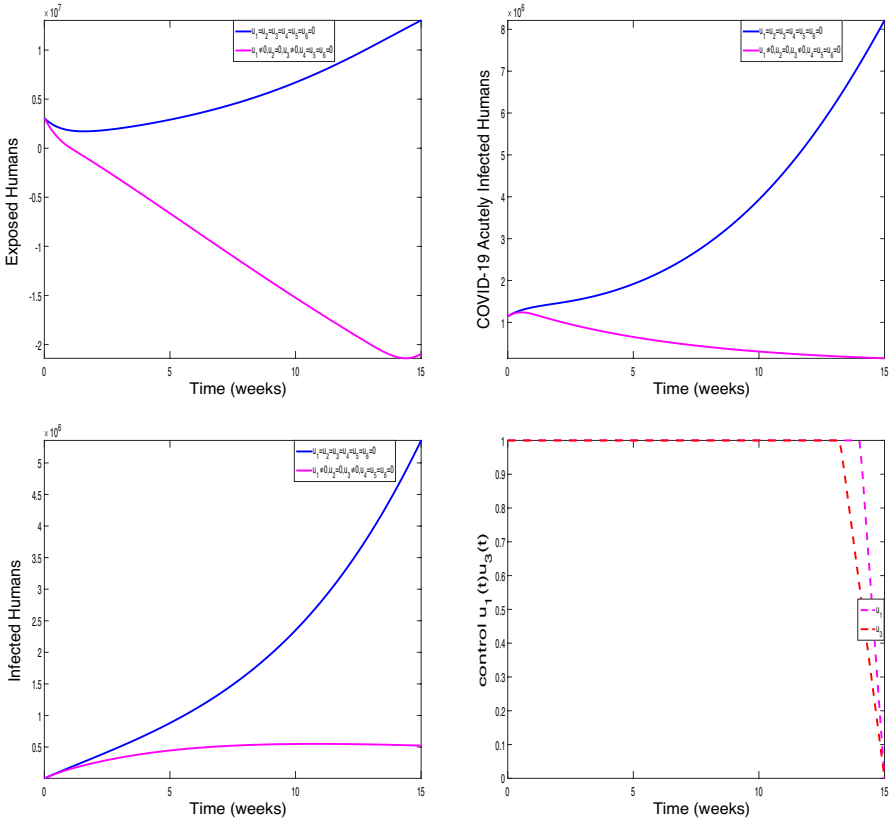

Fig. 8 Effect of scenario A on the COVID-19 dynamics

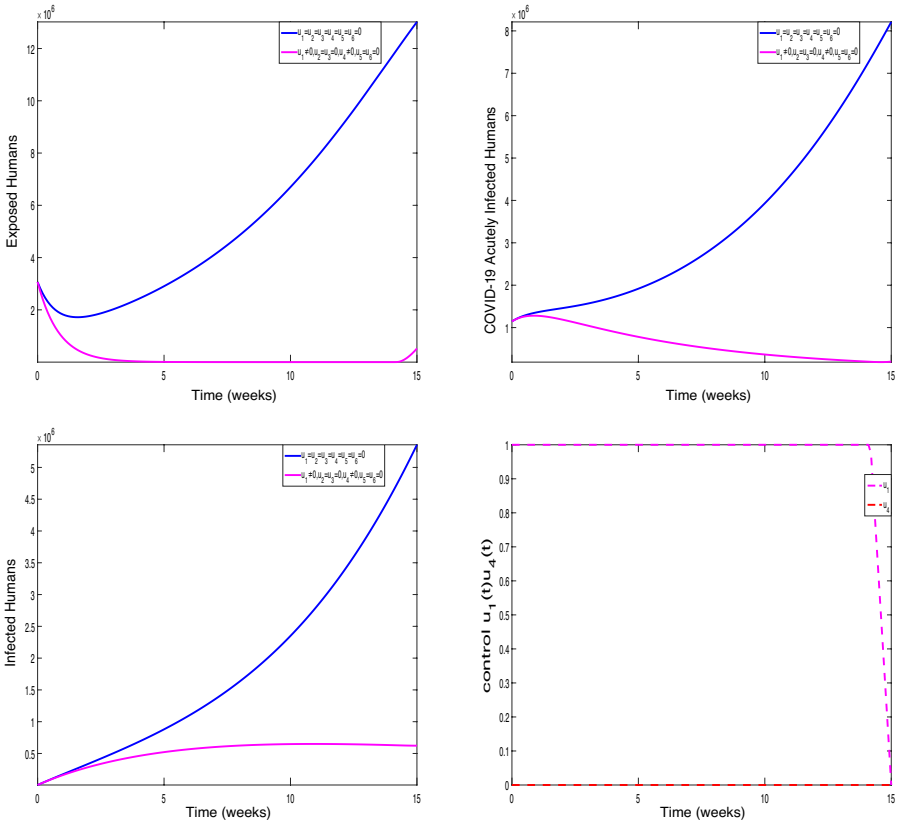

Fig. 9 Effect of scenario B on the COVID-19 dynamics

Figure 8 showcases the effect of implementing Scenario A on the COVID-19 dynamics in the population. It can be seen that as the population increases with time, each population of the exposed, acutely infected humans and infectious humans reduces when controls are deployed in comparison with the situation when control is not assigned. The control profile for Scenario A on the other hand reflects that controls u_1 and u_3 should be upheld at maximum for the first 14th weeks of implementation to the terminal time of implementation so as to truncate the coronavirus transmission effectively in the community. Critically looking at Figs. 9, 10, 11, 12, 13, one sees that similar behaviours are observed for the exposed, acutely infected, and infectious humans, respectively when other combinations of the controls are put into practice while reductions in each population differ. However, It is observed from the control profile for Scenarios B, C, and D that intervention strategies u_1, u_2, and u_3 should be kept up at maximum within the first 14 weeks before retracing infinitesimally to the final implementation period, while optimal implementation of u_4 right from the first day of implementation is encouraged. Furthermore, the control profile for Scenario E reflects that intervention u_6, representing treatment control should be maintained optimally within the first 4 to 5 weeks before retiring to the end time of implementation. In Scenario F, when all the controls are considered, it can be seen that controls u_1, u_2, and u_3 need

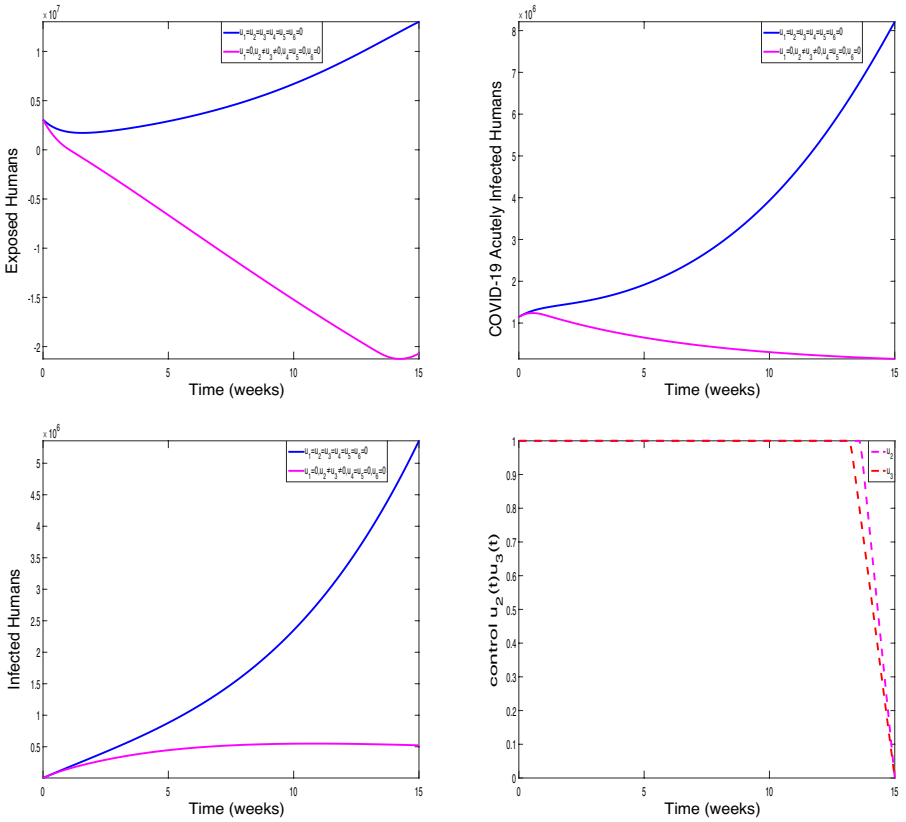

Fig. 10 Effect of scenario C on the COVID-19 dynamics

to be kept at the highest level for approximately 3 weeks of the application period before gradually coming to zero, while u_4 is encouraged to upheld at maximum of 100% throughout the entire implementation time before dropping down to zero. And u_5 and u_6 are maintained at a maximum 100% for a length of time 13 to 14 weeks of the stipulated implementation period before gradually retracing to the terminal implementation period.

7 Conclusion

In an attempt to forestall the lingering threat posed by the coronavirus disease outbreak in the population, a robust nonlinear autonomous mathematical model for the transmission dynamics of coronavirus disease was designed. The designed model categorized the entire population of humans at time t into six epidemiological classes: susceptible population,

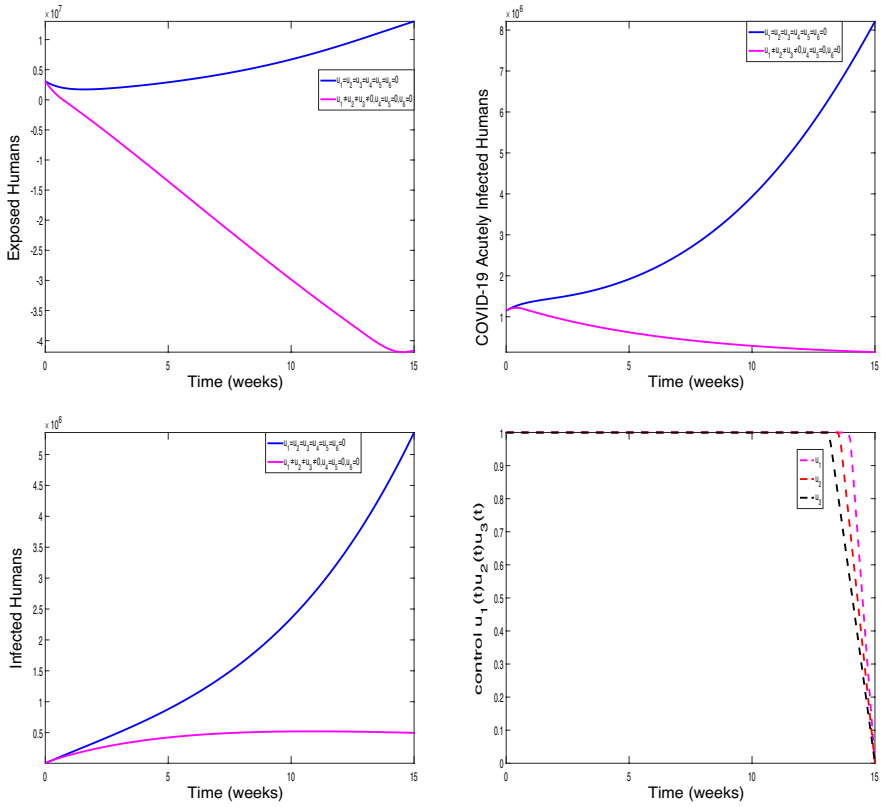

Fig. 11 Effect of scenario D on the COVID-19 dynamics

exposed population, acutely infected population, infectious population, hospitalized population, and recovered population, respectively. Several dynamical system methods were employed to qualitatively and quantitatively analyze the model for more insights into the dynamics of coronavirus transmission in the population.

The model's solutions were proved to be positive and bounded. The threshold parameter responsible for the justification of the existence and stability of the steady states of the COVID-19 model was obtained. In particular, by item 3 of Theorem 4.1, the COVID-19 model will exhibit backward bifurcation, which is a phenomenon where both stable endemic and stable disease-free equilibria co-exist whenever the basic reproduction number of the model is not up to unity. Implying that there will be serious difficulty preventing and controlling COVID-19 spread in the population. Moreover, using the Lyapunov function, the endemic equilibrium point of the COVID-19 model was proved to be globally asymptotically stable whenever the associated reproduction number of the model exceeds unity.

Furthermore, some key epidemiological features like transmission rate, β, modification parameter, η, movement rates, θ, and ψ, responsible for the prevalence of the disease, were identified. As a fallout of this identification, the model was further extended to incorporate

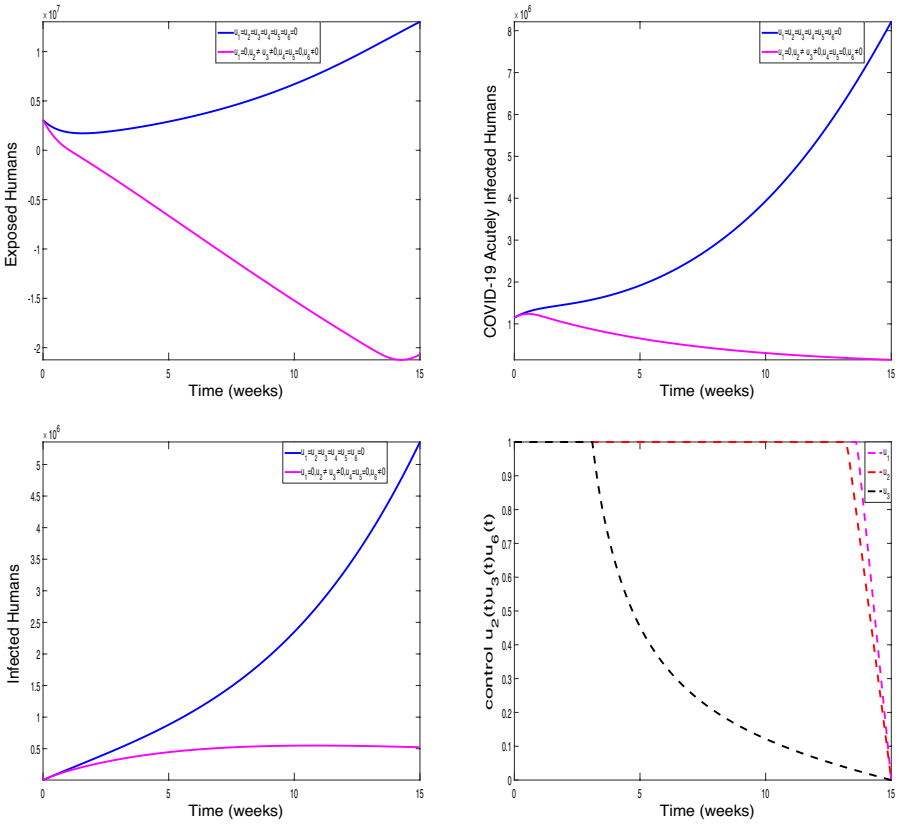

Fig. 12 Effect of scenario E on the COVID-19 dynamics

six time-dependent optimal control interventions, including public education, vaccination with a single dose and second dose, hospitalization and treatment efforts to allow for effective control of the coronavirus spread in the community. The non-autonomous version of the COVID-19 model was analyzed using the celebrated Pontryagin's maximum principle. To significantly reduce the episodes of the SARS-Cov-2 disease, the optimal control sextuple was stratified into different scenarios, combining any two, three, and all the intervention strategies. Consequently, a remarkable cutdown was observed in the COVID-19 prevalence when each control scenario was applied compared to when the scenarios were not implemented. It is important to mention that one of the limitations of this study is that the initial conditions used for the simulations were hypothetical values.

Further simulations of the COVID-19 model revealed that a surge in the values of such parameters as transmission rate, modification parameter that measures the degree of infectiousness of acutely infected individuals, and movement rates would hinder the extinction of COVID-19 in society. Hence, the result of the findings availed in this study suggests that serious attention should be given to such parameters to achieve a COVID-19-free environment. Moreover, by simulating various scenarios and interventions, this work offers valuable insights that can help policymakers craft effective, efficient, and adaptable strategies

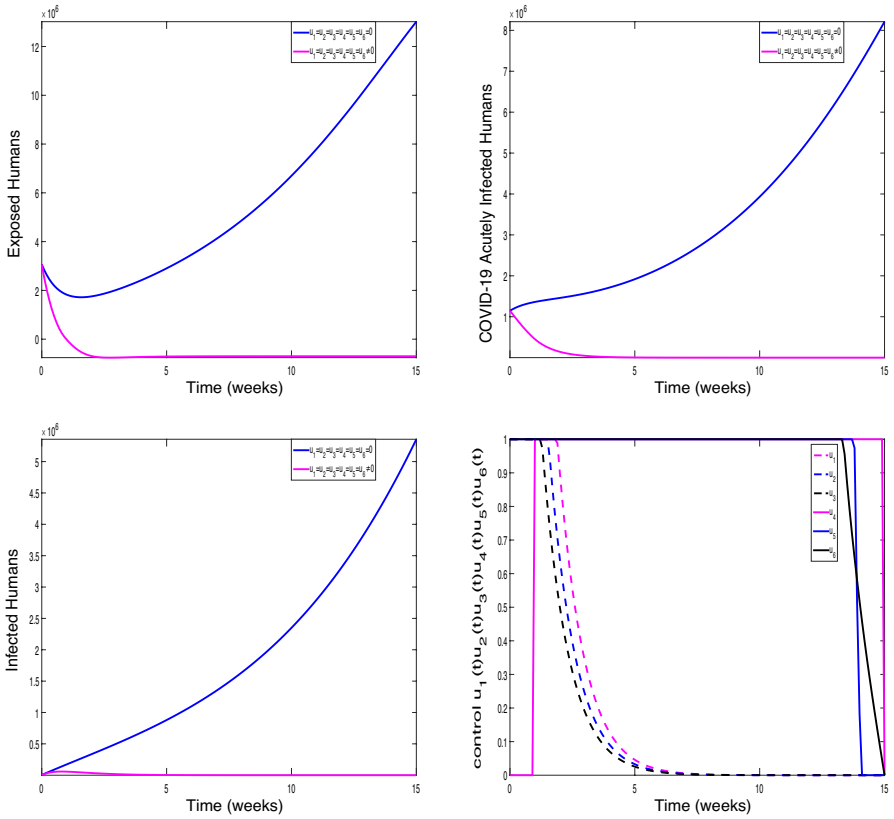

Fig. 13 Effect of scenario F on the COVID-19 dynamics

to mitigate the impact of COVID-19. Specifically, we noticed that the use of these controls: public education, $u_1(t)$, vaccination with a single dose, $u_2(t)$, vaccination with the second dose, $u_3(t)$, an increase in a polymerase chain reaction (PRC) testing equipment, $u_4(t)$, hospitalization rate $u_5(t)$, and treatment rate (prophylaxis) $u_6(t)$ could help policymakers gain insights into protecting the population from another major COVID-19 outbreak. Notably, the parameter values and initial conditions utilized in this research to simulate the COVID-19 model were hypothetically chosen. Nevertheless, real situation data could be used to forecast the possible dynamic patterns of the disease in the community. In addition, we plan to study the dynamics of the disease based on the socio-economic status.

Acknowledgements We sincerely thank the reviewers for their thorough and insightful feedback. Your expertise and detailed evaluations have significantly enhanced the quality of the work. Your dedication and professionalism are truly appreciated.

Author contributions All authors contributed to the study conception and design. Material preparation, analysis and writing of the first draft were performed by J. O. A., S. A and J.K.K.A, Simulation were carried out by J.O.A, S.A. and S.F.A, Supervision, investigation and resource were carried out by J.O.A,S.A, J.K.K.A and F.F.

Funding The authors declare that no funds, grants, or other support were received during the preparation of this manuscript.

Declarations

Conflict of interest The authors have no relevant financial or non-financial interests to disclose.

References

Abidemi, A., Zainuddin, Z.M., Aziz, N.A.B.: Impacts of control interventions on COVID-19 population dynanmics in Malaysia: a mathematical study. Eur. Phys. J. Plus. **136**, 237 (2021)

Abidemi, A., Olaniyi, S., Adepoju, O.A.: An explicit note on the existence theorem of optimal control problem. J. Phys. Conf. Ser. **2199**, 012021 (2022). https://doi.org/10.1088/1742-6596/2199/1/012021

Abidemi, A., Akanni, J.O., Makinde, O.D.: A non-linear mathematical model for analyzing the impact of COVID-19 disease on higher education in developing countries. Healthc. Anal. **3**, 100193 (2023)

Abriham, A., Dengene, D., Abera, T., Elias, A.: Mathematical modelling for COVID-19 transmission dynamics and the impact of prevention strategies: a case study of Ethiopia. Int. J. Math. Sci. Comput. **4**, 43–59 (2021). https://doi.org/10.5815/ijmsc.2021.04.05

Ajao, S., Olopade, I., Akinwumi, T., Adewale, S., Adesanya, A.: Understanding the transmission dynamics and control of HIV infection: a mathematical model approach. J. Niger. Soc. Phys. Sci. **5**(2), 1389 (2023)

Akanni, J.O., Akinpelu, F.O., Olaniyi, S., Oladipo, A.T., Ogunsola, A.W.: Modelling financial crime population dynamics: optimal control and cost-effectiveness analysis. Int. J. Dynam. Control. **8**, 531–544 (2020). https://doi.org/10.1007/s40435-019-00572-3

Asamoah, J.K.K., Owusu, M.A., Jin, Z., Oduro, F.T., Abidemi, A., Gyasi, E.O.: Global stability and cost-effectiveness analysis of COVID-19 considering the impact of the environment: using data from Ghana. Chaos Solitons Fractals **140**, 110103 (2020)

Asamoah, J.K.K., Jin, Z., Sun, G.Q.: Non-seasonal and seasonal relapse model for Q fever disease with comprehensive cost-effectiveness analysis. Results Phys. **22**, 103889 (2021)

Asamoah, J.K.K., Jin, Z., Sun, G.Q., Seidu, B., Yankson, E., Abidemi, A., Okyere, E.: Sensitivity assessment and optimal economic evaluation of a new COVID-19 compartmental epidemic model with control interventions. Chaos Solitons Fractals **146**, 110885 (2021)

Asamoah, J.K.K., Okyere, E., Abidemi, A., Moore, S.E., Sun, Q.: Optimal control and comprehensive cost-effectiveness analysis for COVID-19. Results Phys. **33**, 105177 (2022)

Asamoah, J.K.K., Safianu, B., Afrifa, E., Obeng, B., Seidu, B., Wireko, F.A., Sun, G.Q.: Optimal control dynamics of Gonorrhea in a structured population. Heliyon, **9**(10) (2023)

Awasthi, A.: A mathematical model for transmission dynamics of COVID-19 infection. Eur. Phys. J. Plus. **138**, 285 (2023). https://doi.org/10.1140/epjps/s13360-023-03866-w

Balakrishnan, M., Varadharajan, R.: Spatial patterns and multilevel analysis of factors associated with paediatric tuberculosis in India. Indian J. Tuberc. (2024). https://doi.org/10.1016/j.ijtb.2024.04.014

Castillo-Chavez, C., Feng, Z., Huang, W.: On the computation of R_o and its role on global stability. In: Castillo-Chavez, C., van den Driessche, P., Kirschner, D., Yakubu, A.-A. (eds.) Mathematical approaches for emerging and re-emerging infectious diseases: an introduction, pp. 229–250. Springer-Verlag, Berlin (2002)

Cauchemez, S., Fraser, C., Van Kerkhove, M.D., Donnelly, C.A., Riley, S., Rambaut, A., Enouf, V., van der Werf, S., Ferguson, N.M.: Middle East respiratory syndrome coronavirus: quantification of the extent of the epidemic, surveillance biases, and transmissibility. Lancet Infect Dis. **14**(1), 50–56 (2014). https://doi.org/10.1016/S1473-3099(13)70304-9

Centre for Disease Control and Prevention, COVID-19, https://www.cdc.gov/coronavirus/2019-ncov/index.html, (accessed 18 Jan 2024)

Das, T., Bandekar, S.R., Srivastav, A.K., et al.: Role of immigration and emigration on the spread of COVID-19 in a multipatch environment: a case study of India. Sci. Rep. **13**, 10546 (2023). https://doi.org/10.1038/s41598-023-37192-z

Ferguson, N.M., Laydon, D.J., Gilani, G.N., Imai, N., Ainslie, K.E., Baguelin, M., Bhatia, S., Boonyasiri, A. et al.: Report 9: impact of non-pharmaceutical interventions (NPIs) to reduce COVID-19 mortality and healthcare demand, Imperial College London, (2020). https://doi.org/10.25561/77482

Fleming, W.H., Richel, R.W.: Deterministic and stochastic optimal control. Springer Science & Business Media (2012)

Garba, S.M., Lubuma, J.M., Tsanou, B.: Modeling the transmission dynamics of the COVID-19 Pandemic in South Africa. Math Biosci. **328**, 108441 (2020). https://doi.org/10.1016/j.mbs.2020.108441
Goswami, N.K., Shanmukha, B.: Dynamics of COVID-19 outbreak and optimal control strategies: a model-based analysis. Adv. Syst. Sci. Appl. **21**(4), 65–86 (2021)
Haq, I.U., Ullah, N., Ali, N., Nisar, K.S.: A new mathematical model of COVID-19 with quarantine and vaccination. Mathematics **11**, 142 (2023). https://doi.org/10.3390/math11010142
Hen, Z., Chu, Y., Khan, M.A., Muhammad, S., Al-Hartomy, O.A., Higazy, M.: Mathematical modeling and optimal control of the COVID-19 dynamics. Results Phys. **31**, 105028 (2021). https://doi.org/10.1016/j.rinp.2021.105028
Huang, B., Wang, J., Cai, J., Yao, S., Chan, P.K.S., et al.: Integrated vaccination and physical distancing interventions to prevent future COVID-19 waves in Chinese cities. Nat. Human Behav. **5**, 695–705 (2021)
Idisi, O.I., Yusuf, T.T., Owolabi, K.M., Ojokoh, B.A.: A bifurcation analysis and model of COVID-19 transmission dynamics with post-vaccination infection impact. Healthc. Anal. **3**, 100157 (2023). https://doi.org/10.1016/j.health.2023.100157
Iyaniwura, S.A., Rabiu, M., Jude, D.K.: A generalized distributed delay model of COVID-19: An endemic model with immunity waning. Math. Biosci. Eng. **20**(3), 5379–5412 (2023)
Khan, A.A., Ullah, S., Amin, R.: Optimal control analysis of COVID-19 vaccine epidemic model:a case study. Eur. Phys. J. Plus **137**, 156 (2022). https://doi.org/10.1140/epjp/s13360-022-02365-8
Kifle, Z.S., Obsu, L.L.: Mathematical modeling for COVID-19 transmission dynamics: a case study in Ethiopia. Results Phys. **34**, 105191 (2022). https://doi.org/10.1016/j.rinp.2022.105191
Kouidere, A., Balatif, O., Rachik, M.: Cost-effectiveness of a mathematical modeling with optimal control approach of spread of COVID-19 pandemic: a case study in Peru. Chaos Solitons Fractals X **10**, 100090 (2023). https://doi.org/10.1016/j.csfx.2022.100090
LaSalle, J.P.: The stability of dynamical systems, regional conference series in applied mathematics. SIAM, Philadelphia (1976)
Li, T., Guo, Y.: Optimal control and cost-effectiveness analysis of a new COVID-19 model for Omicron strain. Phys. A Stat. Mech. Appl. **606**, 128134 (2022)
Masandawa, L., Mirau, S.S., Mbalawata, I.S.: Mathematical modeling of COVID-19 transmission dynamics between healthcare workers and community. Results Phys. **29**, 104731 (2021). https://doi.org/10.1016/j.rinp.2021.104731
Mekonen, K.G., Aragaw, F.M., Aknda, K.T.: Optimal control analysis on the impact of non-pharmaceutical interventions and vaccination on the dynamics of COVID-19. Results Control Optim. **13**, 100319 (2023). https://doi.org/10.1016/j.rico.2023.100319
Oke, S.I., Ekum, M.I., Akintande, O.J., Adeniyi, M.O., Adekiya, T.A., Achadu, O.J., Matadi, M.B., Iyiola, O.S., Salawu, S.O.: Optimal control of the coronavirus pandemic with both pharmaceutical and non-pharmaceutical interventions. Int. J. Dynam. Control (2023). https://doi.org/10.1007/s40435-022-01112-2
Okuonghae, D., Omame, A.: Analysis of a mathematical model for COVID-19 population dynamics in Lagos. Niger. Chaos Solitons Fractals **139**, 110032 (2020). https://doi.org/10.1016/j.chaos.2020.110032
Olaniyi, S., Obabiyi, O.S.: Qualitative analysis of malaria dynamics with nonlinear incidence function. Appl Math Sci. **8**(78), 3889–3904 (2014). https://doi.org/10.12988/ams.2014.45326
Olaniyi, S., Obabiyi, O.S., Okosun, K.O., Oladipo, A.T., Adewale, S.O.: Mathematical modelling and optimal cost-effective control of COVID-19 transmission dynamics. Eur. Phys. J. Plus (2020). https://doi.org/10.1140/epjp/s13360-020-00954-z
Olaniyi, S., Ajala, O.A., Abimbade, S.F.: Optimal control analysis of a mathematical model for recurrent malaria dynamics. Oper. Res. Forum. **4**, 14 (2023). https://doi.org/10.1007/s43069-023-00197-5
Paul, A.K., Kuddus, M.A.: Mathematical analysis of a COVID-19 model with double dose vaccination in Bangladesh. Results Phys. **35**, 105392 (2022). https://doi.org/10.1016/j.rinp.2022.105392
Paul, J.N., Mbalawata, I.S., Mirau, S.S., Masandawa, L.: Mathematical modeling of vaccination as a control measure of stress to fight COVID-19 infections. Chaos Solitons Fractals **166**, 112920 (2023). https://doi.org/10.1016/j.chaos.2022.112920
Pontryagin, L.S., Boltyanskii, V.G., Gamkrelidze, R.V., Mishchenko, E.F.: The mathematical theory of optimal processes. Wiley, New York (1962)
Rai, R.K., Tiwari, P.K., Khajanchi, S.: Modeling the influence of vaccination coverage on the dynamics of COVID-19 pandemic with the effect of environmental contamination. Math. Meth. Appl. Sci. **46**(12), 12425–12453 (2023)
Rois, M.A., Fatmawati, F., Alfiniyah, C.: Two isolation treatments on the COVID-19 model and optimal control with public education. Jambura J. Biomath. **4**(1), 88–94 (2023)

Sepulveda, G., Arenas, A.J., Gonzalez-Parra, G.: Mathematical modelling of COVID-19 dynamics under two vaccination doses and delay effects. Mathematics **11**, 369 (2023)
Sharbayta, S.S., Desta, H.D., Abdi, T.: Mathematical modelling of COVID-19 transmission dynamics with vaccination: a case study in Ethiopia. Descrete Dyn. Nat. Soc. **2023**, 2972164 (2023)
Sharma, S., Samanta, G.: Stability analysis and optimal control of an epidemic model with vaccination. Int J Biomath. **8**(3), 1550030 (2015). https://doi.org/10.1142/S1793524515500308
Srivastav, A.K., Ghosh, M., Bandekar, S.R.: Modeling of COVID-19 with limited public health resources: a comparative study of three most affected countries. Eur. Phys. J. Plus. **136**, 359 (2021). https://doi.org/10.1140/epjp/s13360-021-01333-y
Tang, B., Bragazzi, N.L., Li, Q., Tang, S., Xiao, Y., Wu, J.: An updated estimation of the risk of transmission of the novel coronavirus (2019-nCov). Infect. Dis. Modell. **5**, 248–255 (2020). https://doi.org/10.1016/j.idm.2020.02.001
van den Driessche, P., Watmough, J.: Reproduction numbers and sub-threshold endemic equilibria for compartmental models of disease transmission. Math. Biosci. **180**, 29–48 (2002)
Venkatesh, A., Rao, M.A., Vamsi, D.D.: A comprehensive study of optimal control model simulation for COVID-19 infection with respected to multiple variants, Commun. Math. Biol. Neurosci. 75 (2023)
World Health Organization, Coronavirus disease (COVID-19). https://www.who.int/health-topics/coronavirus, 2024 (accessed 18 Jan 2024)
Yang, B., Yu, Z., Cai, Y.: The impact of vaccination on the spread of COVID-19: studying by a mathematical model. Phys. A. **590**, 126717 (2022). https://doi.org/10.1016/j.physa.2021.126717
Zhai, X., Li, W., Wei, F., Mao, X.: Dynamics of an HIV/AIDS transmission model with protection awareness and fluctuations. Chaos Solitons Fractals **169**, 113224 (2023). https://doi.org/10.1016/j.chaos.2023.113224

Authors and Affiliations

J. O. Akanni[1,2] · Fatmawati[2] · S. Ajao[3] · J. K. K. Asamoah[4,5] · S. F. Abimbade[6]

✉ Fatmawati
fatmawati@fst.unair.ac.id

[1] Department of Mathematical and Computing Sciences, Koladaisi University, Ibadan, Oyo State, Nigeria

[2] Department of Mathematics, Faculty of Science and Technology, Universitas Airlangga, Surabaya 60115, Indonesia

[3] Department of Mathematics and Computer Science, Elizade University, Ilara-Mokin, Ondo State, Nigeria

[4] Department of Mathematics, Saveetha School of Engineering SIMATS, Chennai, India

[5] Department of Mathematics, Kwame Nkrumah University of Science and Technology, Kumasi, Ghana

[6] Department of Pure and Applied Mathematics, Ladoke Akintola University of Technology, Ogbomoso, Oyo State, Nigeria